

Properties of Chelating Resins Prepared by Addition of 1,4,8,11-Tetraazacyclotetradecane-5,7-dione to Epoxy Groups of Poly(glycidyl methacrylate)s Crosslinked with Oligoethylene Glycol Dimethacrylates

AKINORI JYO,^{1,*} MASAHIRO SASSA,¹ and HIROAKI EGAWA²

¹Department of Applied Chemistry, Faculty of Engineering, Kumamoto University, and ²Kumamoto Institute of Technology, Kumamoto 860, Japan

SYNOPSIS

In order to improve Cu(II) adsorption ability of chelating resins based on a macrocyclic ligand 1,4,8,11-tetraazacyclotetradecane-5,7-dione (L) bound to crosslinked copolymers, the resins were prepared by reaction of L with poly(glycidyl methacrylate)s crosslinked with ethylene glycol dimethacrylate (1G), tetraethylene glycol dimethacrylate (4G) or non-aethylene glycol dimethacrylate (9G). By systematically changing the amounts of each crosslinker (degree of crosslinking) and of isobutyl acetate (IBA) as diluent in the suspension polymerization of the monomers, precursory copolymers with various degrees of crosslinking as well as with different specific surface areas (SSAs) were prepared, and then L was introduced into them. Ligand contents, SSAs, and Cu(II) adsorption abilities of the resulting resins were evaluated, and it was clarified that resins derived from precursors (prepared by using 4G or 9G in the presence of 120–160 vol % of IBA) exhibit high capacities for Cu(II), whereas the capacities of resins crosslinked with 1G are not so high. Further detailed study on the uptake of metal ions using the resins RG4D(10)-140 and RG9D(10)-140 (derived from the precursors prepared by using 10 mol % of the respective crosslinkers 4G and 9G in the presence of 140 vol % of IBA) showed that RG9D(10)-140 is much superior to RG4D(10)-140 in the column-mode adsorption of Cu(II). These results indicate that not only the selection of the suitable crosslinker but also the use of a pertinent amount of the diluent are very important in improving the complexing abilities of the polymer-bound L.

© 1996 John Wiley & Sons, Inc.

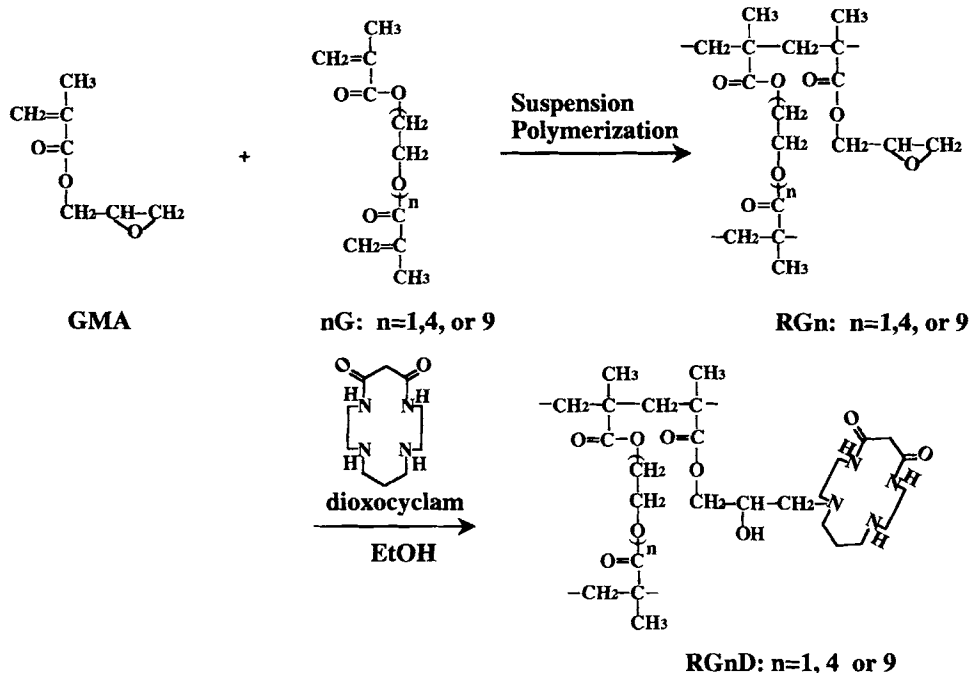
INTRODUCTION

It has been clarified that a macrocyclic ligand, 1,4,8,11-tetraazacyclotetradecane-5,7-dione (dioxocyclam, L), exhibits characteristic complexation and decomplexation reactions^{1–9}; the ligand L exhibits high selectivity toward Cu(II) forming the complex CuLH_{-2} , in which two amide protons are dissociated and decomplexation of CuLH_{-2} with acids occurs through the formation of an iminol intermediate, leading to the extraordinarily rapid acid decomplexation. Thus the chelating resins

containing L are of interest from the viewpoint of the separation of metal ions. However, studies on chelating resins based on L are rare.^{10,11} In a previous paper,¹⁰ we have reported that metal ion uptake by chelating resins containing L is markedly influenced by precursory copolymer species; the resin RGD derived from poly(glycidyl methacrylate-*co*-divinylbenzene) (RG) takes up Cu(II) much more effectively than does the resin RCSD, prepared by reaction of L with chloromethylated poly(styrene-*co*-divinylbenzene) (RCS), indicating that RG is a preferable precursor for the fixation of L to RCS.

Regarding these results, of interest are properties of resins prepared by introduction of L into poly(glycidyl methacrylate) beads crosslinked with

* To whom correspondence should be addressed.



Scheme 1 Preparation of resins RGnD ($n = 1, 4, \text{ or } 9$).

divinyl monomers having hydrophilic bridging moieties (Scheme 1): ethylene glycol dimethacrylate (1G), tetraethylene glycol dimethacrylate (4G), and nonaethylene glycol dimethacrylate (9G). L was introduced to these copolymer beads and properties of the resulting resins were studied.

EXPERIMENTAL

Preparation of Chelating Resins (Scheme 1)

The ligand L was prepared according to the reported method,¹² and was identified by means of CHN analysis, melting point, and proton NMR.

Precursory copolymer beads were prepared by suspension polymerization of glycidyl methacrylate (GMA) and a crosslinker (1G, 4G, or 9G) in the presence of isobutyl acetate (IBA) as diluent (porogen). The diluent IBA was selected, referring to our recent work.¹³ The monomer mixture with a given mol % of the crosslinker was prepared in such a way that the sum of the volumes of the two monomers became 50 mL. After a predetermined volume of IBA and azobisisobutyronitrile (0.5 g) as initiator were added to the monomer mixture, the resulting organic solution was transferred into a 1-L glass autoclave, in which an aqueous solution (500 mL) of sodium sulfate (6 g) and gelatin (0.5 g) was previously taken. The mixture in the autoclave was stirred until the organic solution was dispersed as fine

droplets. The temperature of the suspension was raised to 70°C and maintained for 1 h. During the next 1.5 h, the temperature was raised to 90°C and maintained for 2 h to complete the polymerization. The resulting copolymer beads were filtered off, and the beads were treated in boiling water under stirring. They were then immersed in methanol overnight. After air-drying, the beads were meshed to select those with diameters of 32–60 mesh. By varying compositions of the ternary organic solutions, consisting of GMA, a crosslinker, and IBA, poly(glycidyl methacrylate)s with various degrees of crosslinking as well as with different specific surface areas were prepared. Poly(glycidyl methacrylate)s crosslinked with 1G, 4G, and 9G are abbreviated as RG1(X)-Y, RG4(X)-Y, and RG9(X)-Y, respectively. Here, X means nominal mol % of each crosslinker in the monomer mixture, and Y represents the amount of the diluent designated by (diluent volume/monomer mixture volume) × 100 (vol %). Just before functionalization, the precursory copolymer beads were dried in vacuo at 40°C for more than 1 day.

The introduction of L to copolymer beads was carried out by heating the copolymers and L in the presence of ethanol as reaction solvent in a stainless-steel autoclave at 140°C for 5 h. The weight ratio of copolymer beads, L, and ethanol was 1 : 2 : 4.5. These reaction conditions were determined by the preliminary work on optimization of the ligand in-

roduction. Unless otherwise noted, the weight of each precursory copolymer was 0.3 or 0.4 g. The resulting resin was washed with ethanol in a column until the unreacted L was not detected in the washing. After air-drying, the resulting resins were thoroughly dried in vacuo at 40°C for more than 1 day. All resins were used in the free amine form. The resins derived from RG1(X)-Y, RG4(X)-Y, and RG9(X)-Y are denoted by symbols RG1D(X)-Y, RG4D(X)-Y, and RG9D(X)-Y, respectively.

Properties of Precursory Copolymers and Resulting Chelating Resins

The introduction of the ligand was identified by recording IR spectra of precursors and resulting chelating resins as described in a previous paper.¹⁰ Ligand contents in the resins were calculated from their nitrogen contents. Specific surface areas were measured by means of a BET method using a Shimadzu Flowsorb II apparatus. Volumes of dry and wet resins were measured according to the method reported elsewhere.¹⁴

Batchwise Metal Ion Uptake

Metal ion uptake was evaluated by two approaches. The first approach evaluated the capacity for metal ion uptake: a resin (0.100 g) was taken into a 50-mL flask having a ground joint stopper, then a metal ion solution (0.01M, 30 mL) was added to the flask. After the flask was shaken with a thermostated mechanical shaker at 30°C for 24 h, the resin and aqueous solution were separated. An aliquot of the separated solution was titrated with a standardized 0.01M EDTA solution. From a decrease in the metal ion concentration in the solution, the metal ion uptake per g of dry resin (mmol/g) was calculated.

The second approach evaluated the distribution ratios. Here, 0.0001M solution of each metal ion was used and other conditions were the same as those in the first method. Metal ion concentrations in aqueous phases at adsorption equilibrium were determined by means of ICP-AES. From the decrease in the metal ion concentration in the aqueous phase, a distribution ratio (D) designated by the relation $D = N/C$ was calculated; here N (mmol/g) and C (mmol/mL) stand for amounts of the metal ion in the resin and aqueous phases at the adsorption equilibrium, respectively. Detailed conditions, such as compositions of buffers, appear in the Results and Discussion section.

Rate of Cu(II) Uptake

A resin (0.3 g) and deionized water (45 mL) were taken into a 200-mL three-necked flask equipped with a stirrer. After the temperature of the flask contents reached 30°C, a solution (45 mL, cupric sulfate 0.02M, sodium acetate 0.2M, and acetic acid 0.2M) previously maintained at 30°C was added to the flask under stirring. An aliquot of the stirring solution was then sampled at a pertinent interval and the concentration of Cu(II) in the sampled solution was determined by means of ICP-AES. From the concentration decrease of Cu(II) in the solution, Cu(II) uptake at the sampled time was calculated.

Rate of Cu(II) Desorption

After the adsorption rate study, the Cu(II) adsorbed resin was recovered and centrifuged (3,000 rpm, 15 min). After drying in a desiccator over silica gel, the resin was transferred into the three-necked flask with deionized water (60 mL). After temperature of the mixture in the flask reached 30°C, a 3M hydrochloric acid solution previously maintained at 30°C (30 mL) was added. Subsequent procedures were almost the same as those in the adsorption rate study.

Column-mode Study

The resin RG4D(10)-140 or RG9D(10)-140 (0.5 g) was swollen in water for 24 h and then each resin was transferred into a glass column (inner diameter 0.7 cm, length 16.3 cm); wet volumes (resin bed volume) of RG4D(10)-140 and RG9D(10)-140 were 1.80 and 1.56 mL, respectively. A given volume of a feeding solution containing 1 mM each of Cu(II), Mn(II), Ni(II), and Zn(II) was down-flow supplied to the column. After the column was washed with water or a pertinent buffer, elution of the adsorbed metal ions was carried out by supplying 1M hydrochloric acid to the column. Flow rates of all solutions were adjusted with a peristaltic pump and all column effluents were collected on a fraction collector. Concentrations of metal ions in each fraction were determined by means of ICP-AES. Flow rates are represented by space velocity (h^{-1}), which is designated by ratio of flow rates of solutions (mL/h) to the resin-bed volume (mL). Volumes of solutions supplied to the column are represented by bed volumes (ratio of volume of the supplied solutions to resin bed volume). After the elution of adsorbed metal ions, the resins in the columns were regenerated by feeding 1M sodium hydroxide until the effluent was

chloride free, then the columns were washed with water until the effluent became alkali free. The detailed conditions for column operations appear in the Results and Discussion section.

RESULTS AND DISCUSSION

Ligand Contents

Table I summarizes ligand contents of chelating resins RG1D(10)-Y, RG4D(10)-Y, and RG9(10)-Y, which were derived from precursory copolymers synthesized by fixing the amount of each crosslinker at 10 mol % but changing the amount of the diluent (Y). When Y = 0, the ligand contents are extremely small. The ligand content as high as 1.7 mmol/g was achieved, when Y ≥ 80 for RG1D(10)-Y and when Y ≥ 120 for RG4D(10)-Y and RG9D(10)-Y. Thus the efficiency of the functionalization is strongly influenced by Y. These results clearly mean that some amounts of the diluent should be used in the preparation of precursory copolymers in order to enhance the efficiency of the functionalization reaction.

Table II summarizes ligand contents of RG1D(X)-120, RG4D(X)-140, and RG9D(X)-140, which were derived from the precursors synthesized by fixing Y at 120 or 140 vol % but changing the degree of cross-

Table I Effect of Diluent on Ligand Contents and Specific Surface Areas (SSA) of the Resulting Chelating Resins

Resin	Ligand Content (mmol/g)	SSA (m ² /g)
RG1D (10)-0	0.04	0.0 (0.0)*
RG1D (10)-80	1.78	16.1 (15.1)
RG1D (10)-100	1.73	20.3 (21.9)
RG1D (10)-120	1.66	22.6 (23.4)
RG1D (10)-140	1.68	15.4 (18.7)
RG4D (10)-0	0.11	0.0 (0.1)
RG4D (10)-80	0.97	6.8 (4.1)
RG4D (10)-100	1.37	8.3 (1.0)
RG4D (10)-120	1.74	14.1 (2.8)
RG4D (10)-140	1.74	15.3 (16.2)
RG4D (10)-160	1.76	11.6 (5.7)
RG9D (10)-0	0.55	0.0 (0.0)
RG9D (10)-80	1.44	2.9 (0.0)
RG9D (10)-100	1.53	5.1 (0.1)
RG9D (10)-120	1.77	7.9 (0.1)
RG9D (10)-140	1.73	13.5 (0.0)
RG9D (10)-160	1.69	10.5 (0.0)

* Figures in parentheses are values for precursory copolymers.

Table II Effect of Degree of Crosslinking on Ligand Contents and Specific Surface Areas (SSA) of the Resulting Chelating Resins

Resin	Ligand Content (mmol/g)	SSA (m ² /g)
RG1D (5)-120	1.77	16.1 (14.0) ^a
RG1D (10)-120	1.66	22.6 (23.4)
RG1D (15)-120	1.34	31.0 (31.4)
RG1D (20)-120	1.19	34.0 (36.7)
RG4D (2.5)-140	1.94	3.4 (2.3)
RG4D (5)-140	1.85	12.1 (10.2)
RG4D (10)-140	1.74	15.3 (16.2)
	1.68	12.3 (8.3) ^b
RG4D (15)-140	1.60	15.1 (9.7)
	1.62	14.5 (15.7) ^b
RG4D (20)-140	1.53	19.2 (21.2)
RG9D (5)-140	1.87	14.3 (0.1)
RG9D (10)-140	1.73	13.5 (0.0)
RG9D (15)-140	1.58	14.2 (0.0)
RG9D (20)-140	1.40	18.3 (0.0)

^a Figures in parentheses are values for precursory copolymers.

^b These resins were prepared from precursory copolymers synthesized separate run.

linking (X). The ligand contents decrease with an increase in X, indicating that the steric hindrance in the functionalization reaction increases with an increase in the degree of crosslinking. However, the steric hindrance is markedly relaxed in the functionalization of RG4(X)-140 and RG9(X)-140, compared with that of RG1(X)-120. This means that the longer the bridging moiety of the crosslinkers, the lower the steric hindrance in the functionalization reaction.

Specific Surface Area (SSA)

Tables I and II also show SSAs before and after functionalization. When Y = 0, the resins RG1D(10)-0, RG4D(10)-0, and RG9D(10)-0 do not have measurable SSA and can be classified as gel-type resins. SSAs of the RG1D(X)-Y are nearly equal to those of corresponding precursors RG1(X)-Y, suggesting that the functionalization reaction does not bring a significant change in macropore structures of the precursors RG1(X)-Y. In the series RG1D(10)-Y, the largest SSA was observed at Y = 120 (Table I), whereas SSA of the series RG1D(X)-120 simply increases with an increase in X (Table II). Similar tendencies are also observed in SSAs of other kinds of chelating resins derived from macroreticular GMA-divinylbenzene copolymer beads.¹³

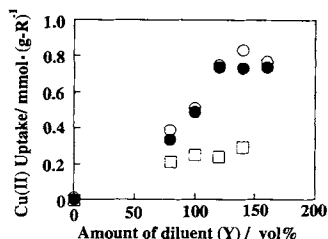


Figure 1 Effect of diluent on uptake of Cu(II). 0.1 g of (□) RG1D(10)-Y, (●) RG4D(10)-Y, or (○) RG9D(10)-Y; 30 mL of solution containing CuSO₄ (0.01M), CH₃COOH (0.1M), and CH₃COONa (0.1M); pH 4.6–4.7; shaking for 24 h at 30°C.

In the functionalization of the precursors RG9(X)-Y, on the other hand, an interesting phenomenon was observed: the precursors RG9(X)-Y do not have measurable SSAs, but the functionalized resins RG9D(X)-Y exhibit measurable SSAs except where $Y = 0$. As is described in the previous section, the efficiency of the ligand introduction is strongly affected by Y and the high ligand contents are achieved when $Y \geq 120$. This implies that some kinds of macropores appear during the functionalization reaction, suggesting that the diluent IBA gives loose macropore structures to RG9(X)-Y ($Y \neq 0$) during the polymerization process. These loose macropores apparently disappear during the drying process, since it seems that long and flexible crosslinking bridges may be not suitable for the formation of stable and rigid macropore structures. However, the apparently disappeared macropores are recovered in the functionalization process by their swelling with ethanol at the elevated temperature (140°C), resulting in the marked dependence of the ligand introduction efficiency on Y (Table I); and measurable SSAs of RG9D(X)-Y also imply that the functionalization reaction changes the loose macropore structures to stable and rigid ones by secondary crosslinking caused by the addition of the ligand's two amino groups to epoxy groups in separate polymer chains. Indeed, even the highest ligand content of 1.94 mmol/g in Tables I and II is much less than the calculated contents based on the ideal 1 : 1 addition of the ligand to each epoxy group (e.g., 2.6 mmol/g for RG4D(2.5)-140).

Last, we refer to SSAs of RG4(X)-Y and RG4D(X)-Y. SSAs of precursors RG4(X)-Y cannot be simply correlated to X or Y and are rather scattered. The effect of the diluent on SSAs of RG4(X)-Y seems to be much more complicated, since the situation is intermediate between the two extreme cases of RG1(X)-Y and RG9(X)-Y. Indeed, the precise control of SSAs of RG4(X)-Y was difficult to

achieve. However, the scattering of SSAs is reduced to some extent by the functionalization reaction.

Uptake of Cu(II) by RG1D(X)-Y, RG4D(X)-Y, and RG9D(X)-Y

Figure 1 shows uptake of Cu(II) by RG1D(10)-Y, RG4D(10)-Y, and RG9D(10)-Y. The Cu(II) uptake is affected not only by the ligand contents but also by other factors, such as crosslinker species and degree of crosslinking. For example, ligand contents of RG1D(10)-0, RG4D(10)-0, and RG9D(10)-0 are 0.04, 0.11, and 0.55 mmol/g, respectively, but these resins hardly take up Cu(II). Furthermore, RG1D(10)-Y ($Y = 80$ –140), RG4D(10)-Y ($Y = 120$ –160), and RG9D(10)-Y ($Y = 120$ –160) have nearly equal ligand contents of ca. 1.7 mmol/g, but RG1D(10)-Y ($Y = 80$ –140) cannot effectively take up Cu(II) compared with RG4D(10)-Y ($Y = 120$ –160) or RG9D(10)-Y ($Y = 120$ –160). These results mean that *precursors prepared by using 4G or 9G as crosslinker in the presence of 120–160 vol % of the diluent are desirable for the preparation of the chelating resins having high capacities for uptake of Cu(II)*.

Figure 2 shows the effect of the degree of crosslinking on the Cu(II) uptake. The Cu(II) uptake by RG1D(X)-120, RG4D(X)-140, and RG9D(X)-140 decreases with an increase in X . Concerning the uptake of Cu(II) by RG4D(X)-140 or RG9D(X)-140, the decrease in the Cu(II) uptake with the increase in X is not marked; it seems that this tendency corresponds to a decrease in the ligand contents with the increase in X (Table II). The Cu(II) uptake of RG1D(X)-120, however, markedly decreases with an increase in X and this marked decrease is not simply explained by the decrease in the ligand content; the polymer matrices crosslinked with the short bridging moiety at high density seem to bring serious steric hindrance in the complexation of the fixed ligand

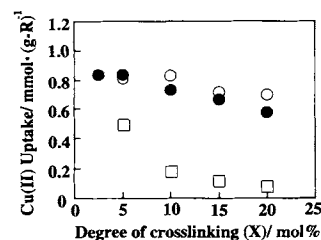


Figure 2 Effect of degree of crosslinking on uptake of Cu(II). 0.1 g of (□) RG1D(X)-120, (●) RG4D(X)-140, or (○) RG9D(X)-140; 30 mL of solution containing CuSO₄ (0.01M), CH₃COOH (0.1M), and CH₃COONa (0.1M); pH 4.6–4.7; shaking for 24 h at 30°C.

Table III Properties of Chelating Resins Used in Detailed Study on Metal Ion Uptake

Resin	Ligand Content (mmol/g)	Specific Surface Area ^a (m ² /g)	Dry Volume (cm ³ /g)	Wet Volume ^b (cm ³ /g)	Uptake of Cu(II) ^b (mmol/g)
RG1D(10)-120	1.66	22.6 (23.4)	2.45	3.20	0.18
RG4D(10)-140	1.68	15.1 (16.2)	2.71	4.39	0.66
RG9D(10)-140	1.69	15.0 (0.0)	2.00	4.01	0.81
RGD(10)-140 ^c	1.55	36.2 (45.3)	2.45	3.11	0.32

^a Figures in parentheses are values for precursors.

^b After shaking in acetic acid-sodium acetate buffer (0.1M of each) at 30°C for 24 h.

^c Derived from glycidyl methacrylate-divinylbenzene copolymer beads synthesized by using 10 mol % of divinylbenzene and 140 vol % of the diluent.

with Cu(II) and/or high resistance for diffusion of Cu(II) in the bulk of the resin phase.

Metal Ion Uptake by Selected Resins

Referring to the results described so far, RG1D(10)-120, RG4D(10)-140, and RG9D(10)-140 were selected as the resins for further detailed study on metal ion uptake, and were prepared on a rather large scale (precursor 4 g). Their properties are summarized in Table III. For comparison, Table III also shows properties of RGD(10)-140, which was derived from the functionalization of glycidyl methacrylate-divinylbenzene copolymer beads prepared using 10 mol % of divinylbenzene and 140 vol % of IBA. Hereafter, the suffixes (10)-120 and (10)-140 are omitted from the resin symbols in the text.

Ligand contents as well as SSAs were nearly equal to those prepared in a small scale (Tables I and II), indicating the high reproducibility of the resin preparation. Although the dry and wet volumes of the resins themselves are not simply correlated to crosslinker species, ratios of wet volumes to dry volumes (swelling ratios) increase with an increase in the number of ethylene glycol unit in the crosslinkers, as expected: swelling ratios of RG1D, RG4D, and RG9D are 1.3, 1.6, and 2.0, respectively. The swelling behavior of RG1D is very close to that of RGD, indicating that 1G is not effective in enhancing the hydrophilicity of the resulting resins. Although the ligand contents of the four resins are nearly equal, the uptake of Cu(II) is strongly affected by the crosslinker species. From the results shown in Table III, as well as in Figures 1 and 2, the Cu(II) uptake increases in the order RG1D < RGD < RG4D ≤ RG9D. Surprisingly, the Cu(II) uptake with RG1D is appreciably less than that of RGD. This is probably due to the difference in SSA between RG1D and RGD, since the great difference is not observed

either in the ligand contents or in swelling behavior between RG1D and RGD. SSA of RGD is much greater than that of RG1D.

Figure 3 shows the time course of the Cu(II) uptake by RG1D, RG4D, and RG9D. Although the three resins exhibit the similar time courses, within 20 min, the rate of the Cu(II) uptake with RG1D markedly slows after 20 min. This means that the Cu(II) uptake by RG1D consists of rapid and slow processes. The rapid process is ascribable to the Cu(II) uptake by the ligand located near the surfaces of microgels; the slow one may correspond to the uptake by the ligand located in the bulk of the microgels, since the lesser swelling of RG1D is not suitable for the rapid diffusion of Cu(II) in the bulk of the microgels. The Cu(II) uptake by RG4D and RG9D, on the other hand, smoothly increased with time. RG9D takes up Cu(II) more rapidly than RG4D does, even though the difference is not marked. With their macroreticular structures, RG4D and RG9D swell more highly than does RG1D

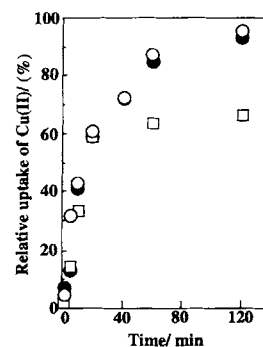


Figure 3 Time course of Cu(II) uptake. The coordinate represents relative uptake to equilibrium one (24 h). Conditions: 0.3 g of (□) RG1D(10)-120, (●) RG4D(10)-140, or (○) RG9D(10)-140; 90 mL of solution containing CuSO₄ (0.01M), CH₃COOH (0.1M), and CH₃COONa (0.1M); pH 4.6–4.7; stirring 170 rpm; temperature 30°C.

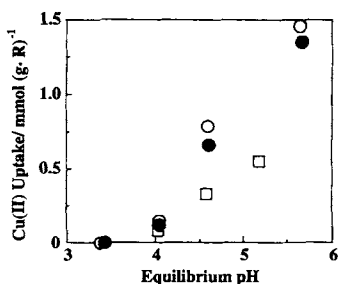


Figure 4 Effect of pH on Cu(II) uptake (capacity). 0.1 g of (□) RGD(10)-140, (●) RG4D(10)-140, or (○) RG9D(10)-140; 30 mL of solution containing CuSO₄ (0.01M); shaking for 24 h at 30°C. The pH of solution was adjusted with acetic acid and/or sodium acetate; values for RGD(10)-140 are quoted from Jyo and co-workers.¹⁰

(Table III). The high swelling brings the rapid diffusion of Cu(II) even in the bulk of the microgels, thus RG4D and RG9D exhibit faster Cu(II) uptake than RG1D. Referring to the kinetic results, the further detailed study is mainly limited to RG4D and RG9D.

It has been reported that the present ligand itself is highly selective to Cu(II) among common divalent transition metal ions.¹⁻⁹ Adsorption of Cd(II), Cu(II), Ni(II), Mn(II), Pb(II), and Zn(II) with RG4D and RG9D was examined in the pH range from 1 to 5 by means of two batchwise approaches (see Experimental section). The metal ions other than Cu(II) were hardly adsorbed under the tested conditions, indicating that the polymer bound L still maintains high selectivity toward Cu(II). Accordingly, the results for Cu(II) only are shown in Figures 4 and 5 and compared with those of RGD.¹⁰ From the data

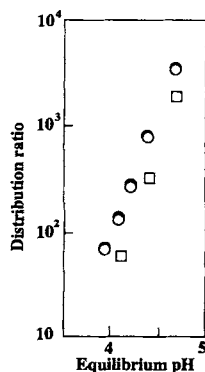


Figure 5 Effect of pH on Cu(II) uptake (distribution ratio). 0.1 g of (□) RGD(10)-140, (●) RG4D(10)-140, or (○) RG9D(10)-140; 30 mL of solution containing CuSO₄ (0.0001M); shaking for 24 h at 30°C. The pH of solution was adjusted with acetic acid and/or sodium acetate; values for RGD(10)-140 are quoted from Jyo and co-workers.¹⁰

Table IV Batchwise Elution of Cu(II) Adsorbed on RG9G*

Concentration of HCl (M)	Cu(II) Eluted (%)
1	100
0.1	100
0.01	61
0.001	4

* To 0.1 g of RG9D, Cu(II) was loaded (1.33–1.34 mmol/g). After removing the mother liquor by centrifugation, the Cu(II)-loaded resin was shaken with 30 mL of eluting solution for 24 h at 30°C.

in these two figures it can be clearly concluded that RG4D and RG9D exhibit much more excellent adsorption of Cu(II) than does RGD. Interestingly, the meaningful difference in distribution ratios for Cu(II) was not observed between RG4D and RG9D (Fig. 5), whereas RG9D exhibits slightly higher capacities for Cu(II) than does RG4D (Fig. 4).

Besides the high performances in the adsorption of metal ions, the adsorbed metal ions should be eluted rapidly and quantitatively, from practical viewpoints. Thus we examined elution of the adsorbed Cu(II). Table IV gives results for batchwise elution of Cu(II) adsorbed on RG9D with hydrochloric acid solutions of four different concentrations. When the acid concentration is higher than 0.1M, the adsorbed Cu(II) is quantitatively eluted. Hay and colleagues have reported that decomplexation of the Cu(II) complex of dioxocyclam (CuLH₂) with proton is extraordinarily rapid compared with Cu(II) complexes of the usual macrocyclic polyamines.³ We also examined the rates of the elution with 1M hydrochloric acid; results are shown

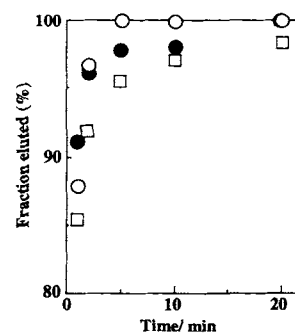


Figure 6 Time course of Cu(II) desorption. Cu(II)-loaded resins obtained in the uptake rate study (Fig. 3) were used. (□) RG1D(10)-120, (●) RG4D(10)-140, or (○) RG9D(10)-140; 90 mL of 1M hydrochloric acid; stirring 170 rpm; temperature 30°C.

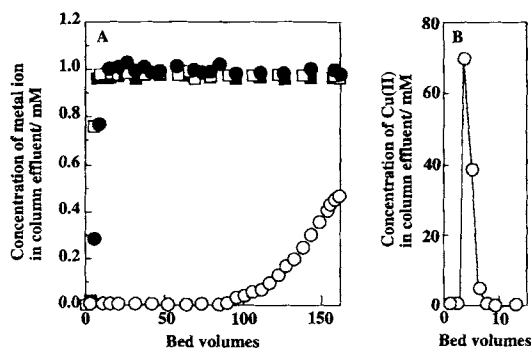


Figure 7 Column-mode adsorption from the pH-buffered feed and elution of the adsorbed metal ions. Column RG9D(10)-140. (A) Adsorption; solution containing 1 mM each of four metal ions was fed at a space velocity of 2.7 h⁻¹. The pH of the solution was fixed at 4.6 with CH₃COOH and CH₃COONa (0.1M of each). (B) Elution; 1M hydrochloric acid was fed at a space velocity of 2.6 h⁻¹. (○) Cu(II), (■) Mn(II), (●) Ni(II), (□) Zn(II).

in Figure 6. Compared with the adsorption rates (Fig. 3), elution rates were very rapid. The times required for the quantitative elution were 5 and 20 min for RG9D and RG4D, respectively. The extremely rapid elution rate of Cu(II) is also one of the outstanding properties of RG9D and RG4D.

Column-mode Study

Performances of RG4D and RG9D in column-mode adsorption were investigated by evaluating breakthrough behavior for feeds, in which 1 mM each of Cu(II), Mn(II), Ni(II), and Zn(II) were simultaneously contained. As feeds, pH-buffered and unbuffered solutions were used.

When the pH of the feed was maintained at 4.6 with an acetic acid-sodium acetate buffer, only Cu(II) was adsorbed, as expected from the batchwise study. Figure 7 shows a typical example of breakthrough and elution curves obtained using the RG9D column; Cu(II) was not leaked until ca. 90 bed volumes of the feed, whereas Mn(II), Ni(II), and Zn(II) were not adsorbed at all. The adsorbed Cu(II) was rapidly and quantitatively eluted within ca. 8 bed volumes of 1M hydrochloric acid, and naturally Mn(II), Ni(II), and Zn(II) were not detected in any fraction of the eluted solution. The RG4D column gave similar results concerning the selectivity of the metal ion adsorption, but the leaking of Cu(II) occurred at smaller bed volumes of the feed. We then examined the effect of the flow rate of the feed; Figure 8 summarizes those results. Here, breakthrough curves for Mn(II), Ni(II), and Zn(II) are omitted, since they are not adsorbed. With increasing flow

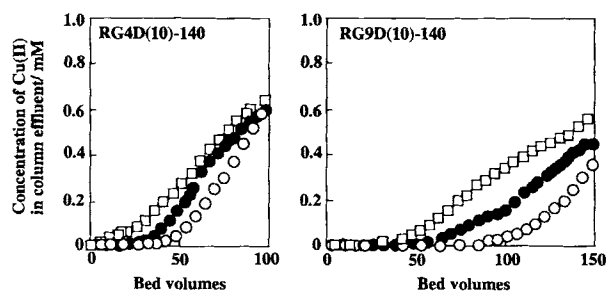


Figure 8 Effect of flow rate on column-mode adsorption of Cu(II). For the composition of the feed, see Figure 7 caption. Flow rate: (○) 2.7 h⁻¹, (●) 4.4 h⁻¹, (□) 10.3 h⁻¹ for RG4D(10)-140; (○) 2.7 h⁻¹, (●) 5.1 h⁻¹, (□) 10.4 h⁻¹ for RG9D(10)-140.

rate, the breakthrough point of Cu(II) decreases. This tendency is more marked for RG4D than for RG9D; this is ascribable to the difference in the Cu(II) adsorption kinetics between the two resins (Fig. 3). It seems, however, that the difference in the rates in the column-mode adsorption is more marked than the one predicted from Figure 3. It is likely that the difference in the adsorption rate is enhanced in the column-mode adsorption, since column operations were carried out at rather lower temperatures (ambient conditions, 15°–20°C).

In the adsorption from the unbuffered conditions (pH 5.3), the Cu(II) breakthrough capacity is greatly enhanced, as shown in Figure 9. The breakthrough point of Cu(II) is at ca. 170 bed volumes of the feed, which is twice that shown in Figure 7. In addition, the breakthrough behaviors for Zn(II) and Ni(II) are also quite different from that shown in Figure 7. The concentration of Zn(II) in the column effluent

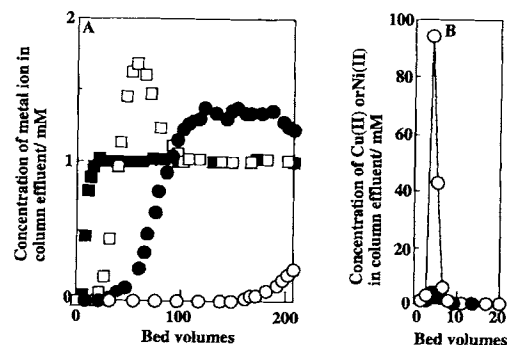


Figure 9 Column-mode adsorption from the unbuffered feed and elution of the adsorbed metal ions. Column RG9D(10)-140. (A) Adsorption; solution containing 1 mM each of four metal ions was fed at a space velocity of 2.7 h⁻¹. (B) Elution; 1M hydrochloric acid was fed at a space velocity of 2.7 h⁻¹. (○) Cu(II), (■) Mn(II), (●) Ni(II), (□) Zn(II).

from 40 to 90 bed volumes exceeds that in the feed, and a similar phenomenon is observed for Ni(II) after 90 bed volumes. However, Mn(II) is not adsorbed even from the nonbuffered solution. These results mean that the selectivity of RG9D toward the four metal ions increases in this order: Mn(II) < Zn(II) < Ni(II) < Cu(II). Since the conditional stability constants of complex MLH_2 increase with increasing pH, even Zn(II) and Ni(II) can be adsorbed in the initial stage of the feeding. On further feeding, however, Zn(II) is replaced by the more-preferred Ni(II) and/or Cu(II), and then Ni(II) by the most-preferred Cu(II). In this experiment Ni(II) is not completely replaced by Cu(II), as judged from the breakthrough curve of Ni(II). Then, a small amount of Ni(II) was detected in the eluted solution, whereas Zn(II) and Mn(II) were not detected. The highest concentration of Cu(II) on the elution curve in Figure 9 is 94 mM, which is greater than that in the feed by ca. 2 orders of magnitude. Thus the presented resins will be useful for the selective separation and concentration of Cu(II). Similar results were obtained for the RG4D column, whereas the breakthrough point of Cu(II) is located at 90 bed volumes of the feed under the column operating conditions given in the legend of Figure 9. During the column-mode experiments, adsorption–elution–regeneration cycles were repeatedly tested and no deterioration of the resins was observed. The column-mode study has also revealed that the resins developed in this work, in particular RG9D, exhibit much higher performances in Cu(II) uptake than does RGD.¹⁰

CONCLUSION

From poly(glycidyl methacrylate)s crosslinked with ethylene glycol dimethacrylate (1G), tetraethylene glycol dimethacrylate (4G), or nonaethylene glycol dimethacrylate (9G), chelating resins containing 1,4,8,11-tetraazacyclotetradecane-5,7-dione (L) were derived. By systematically changing the amounts of each crosslinker and isobutyl acetate as diluent in the preparation of precursory copolymers, chelating resins with various degrees of crosslinking as well as different specific surface areas were derived. In order to enhance the adsorption ability for Cu(II), the precursors should be prepared in the presence of more than 100 vol % of the diluent per the monomeric mixture, even if the precursors do

not have BET-active specific surface areas. The adsorption ability for Cu(II) is greatly influenced by the crosslinker species; the crosslinkers 4G and 9G yield resins with much greater capacities for Cu(II) than does 1G. Among the resins prepared in this work, RG9D(10)-140 derived from the precursor, which was prepared by using 10 mol % of 9G and 140 vol % of the diluent, exhibits the highest performances in both the batchwise and columnar adsorption of Cu(II), indicating that not only the selection of the suitable crosslinker but also the use of the pertinent amount of the diluent is very important in improving performances of the resins containing L.

This work was supported by the Ministry of Education, Science, and Culture of Japan (Grant No. 05650902). The authors thank Nihonyushi Co. Ltd. (Tokyo, Japan) for supplying the glycidyl methacrylate used in this work.

REFERENCES

1. M. Kodama and E. Kimura, *J. Chem. Soc., Dalton Trans.*, **1979**, 325.
2. R. Machida, E. Kimura, and M. Kodama, *Inorg. Chem.*, **22**, 2055 (1983).
3. R. W. Hay, M. P. Pujari, and F. McLaren, *Inorg. Chem.*, **23**, 3033 (1984).
4. E. Kimura, T. Koike, R. Machida, R. Nagai, and M. Kodama, *Inorg. Chem.*, **23**, 4181 (1984).
5. E. Kimura, R. Machida, and M. Kodama, *J. Am. Chem. Soc.*, **106**, 5497 (1984).
6. L. Fabbrizzi, F. Forlini, A. Perotti, and B. Seghi, *Inorg. Chem.*, **23**, 807 (1984).
7. L. Fabbrizzi, T. A. Kaden, A. Perotti, B. Seghi, and L. Siegfriet, *Inorg. Chem.*, **25**, 321 (1986).
8. E. Kimura, S. Korenari, M. Shionoya, and M. Shiro, *J. Chem. Soc., Chem. Commun.*, **1988**, 1166.
9. E. Kimura, T. Koike, T. Shiota, and Y. Iitaka, *Inorg. Chem.*, **29**, 4621 (1990).
10. A. Jyo, I. Hiwatashi, R. Weber, and H. Egawa, *Anal. Sci.*, **8**, 195 (1992).
11. A. Jyo, R. Weber, and H. Egawa, *Anal. Sci.*, **9**, 599 (1993).
12. I. Tabushi, Y. Taniguchi, and H. Kato, *Tetrahedron Lett.*, **1977**, 1049.
13. H. Egawa, A. Jyo, and C. Chen, *Nippon Kagaku Kaishi*, **1994**, 442.
14. H. Egawa, M. Nakayama, T. Nonaka, H. Yamamoto, and K. Uemura, *J. Appl. Polym. Sci.*, **34**, 1557 (1987).

Received May 1, 1995

Accepted June 16, 1995